

MASTER

PREPRINT UCRL-79779

CONF 771136 - 1

Lawrence Livermore Laboratory

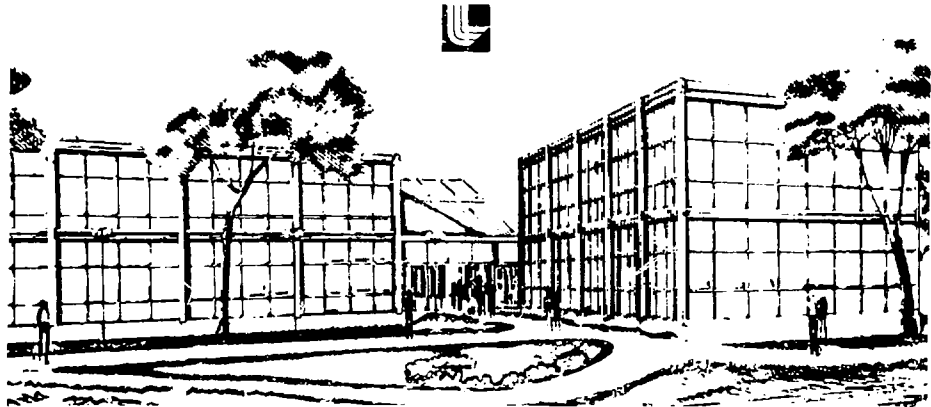
LONG PULSE MICROSPHERE EXPERIMENTS AT 3 TW

M. J. Boyle, D. T. Attwood, K. M. Brooks, E. M. Campbell, L. W. Coleman, L. N. Koppel, H. N. Kornblum, J. T. Larsen, P. H. Y. Lee, D. W. Phillion, R. H. Price, V. C. Rupert, V. W. Slivinsky, E. K. Storm and K. G. Tirsell

November 1, 1977

This paper was prepared for submission to the APS Plasma Meeting of the American Physical Society, Atlanta, Georgia, November 5-11, 1977.

This is a preprint of a paper intended for publication in a journal or proceedings. Since changes may be made before publication, this preprint is made available with the understanding that it will not be cited or reproduced without the permission of the author.



DISTRIBUTION OF THIS DOCUMENT IS UNLIMITED

Abstract Submitted
for the APS Plasma Physics Meeting of the
American Physical Society

November 5-11, 1977

Physics and Astronomy
Classification Scheme
Number 52

Bulletin Subject Heading in
which Paper should be placed
Transport Phenomena, Hydro-
dynamics, and Thermonuclear
Burn

Large Diameter, Long Pulse Exploding Pusher Target
Experiments at 3 TW. M. J. Boyle, D. T. Attwood, K. M. Brooks, E. M. Campbell, L. W. Coleman, L. N. Koppel, H. N. Kornblum, J. T. Larsen, P. H. Y. Lee, D. W. Phillion, R. H. Price, V. C. Rupert, V. W. Slivinsky, E. K. Storm and K. G. Tirsell, Lawrence Livermore
Laboratory. **--Previous 1.06 μm laser implosion experiments have explored the parameter space associated with microsphere targets of typically less than 100 psec. Exploding pusher experiments have now been performed using long pulses (100-200 psec FWHM), and large diameter (100-150 μm) targets on the 3 TW Argus laser facility. Absorption, transport, implosion and neutron and α yield characteristics are discussed and compared with earlier short pulse results. The observed neutron yields are discussed in light of the temporal mismatch between the absorption and implosion time scales imposed by the large diameter, long pulse conditions.

**Supported by U. S. ERDA Contract W-7405-ENG-48

NOTICE
This report was prepared as an account of work sponsored by the United States Government. Neither the United States Government nor the State, Department of Energy, nor any of their employees, nor any of their contractors, subcontractors, or their employees, makes any warranty, express or implied, or assumes any legal liability or responsibility for the accuracy, completeness or usefulness of any information, apparatus, product or process disclosed, or represents that its use would not infringe privately owned rights.

Submitted by

Michael J. Boyle
Michael J. Boyle
University of California
Lawrence Livermore Laboratory
P. O. Box 808, L-549
Livermore, CA 94550

RCR

DISTRIBUTION OF THIS DOCUMENT IS UNLIMITED

LONG PULSE MICROSPHERE EXPERIMENTS AT 3 TW

A series of thin walled, large diameter spherical targets were recently irradiated at the Argus laser fusion facility. Two f/1 aspheric lenses focused approximately 3 TW of 1.06 μm light tangentially down to 100 - 150 μm diameter microsphere targets. Gaussian pulse widths (FWHM) between 150 and 200 ps were employed. These experiments represented a significant departure from previous high power, short pulse exploding pusher experiments at LLL where the incident power was delivered in times between 30 and 80 ps. These experiments extended the pulse duration of exploding pusher parameter space investigated to date at LLL. In particular, a "non-optimized" exploding pusher target regime was examined.

Figure 1 summarizes and compares the parameters and pertinent results of the previous short pulse, small diameter and recent long pulse, large diameter experiments. The remainder of this text reports in more detail the results comparing the absorption characteristics, the neutron yields and the energy loss (or gain) of the thermonuclear alpha particles generated within the compressed core of the imploded microspheres.

Figure 2 compares the absorption fraction for microsphere targets as a function of pulse width. These absorption data result from a variety of techniques including energy balance from discrete Si PIN diode scattered light detectors, plasma calorimeters and near 4π scattered 1.06 μm light calorimetry (box calorimeter). Similar f/1 focusing optics and tangential marginal ray focusing strategies were used for all these experiments. The absorption fraction is seen to decrease by approximately a factor of two as one goes to the longer pulse lengths. Absorption fractions of 10% at these longer pulse widths are indicated.

This trend is accompanied by an increased red shifting of the backreflected (into focusing lens) 1.06 μm spectrum. While the backreflected spectrum has not

yet been directly measured for a short pulse, spherical target, planar targets irradiated at similar intensities and with short pulses, exhibit primarily blue shifted spectra. In contrast, the typical long pulse backreflected spectra from spherical targets, illustrated in Figure 3, appear to be nearly 80% red shifted. The long pulse conditions are favorable for formation of long density gradients in the underdense plasma, which in turn encourage stimulated Brillouin scattering (SBS). The lower observed absorptions and the red shifted reflectivity spectra are consistent with SBS playing a significant role in these long pulse experiments.

Figure 4 plots the long pulse, large ball neutron yields against the absorbed specific energy and compares them with other short pulse results. Variations in target geometry, that is to say microsphere diameter and wall thickness, have been accounted for by the normalizations indicated. The solid line basically represents the neutron dependence upon the Maxwellian averaged DT thermonuclear cross section assuming the ion temperature is proportional to the absorbed specific energy. Clearly, the normalized, long pulse yields do not fall along the curve. It has been demonstrated that a simple scaling model, the fundamentals of which are presented in Figure 5, is able to better correlate the apparent variations in neutron yield for exploding pusher microsphere targets. The model postulates a simple relationship between the laser energy absorption times and the hydrodynamic implosion times. Obviously, laser absorption after the implosion of the microsphere target can no longer contribute to the increase in thermonuclear events. The more exact specification of this laser absorption "cutoff" time results in the definition of "useful" rather than "absorbed" specific energy. Upon replotted the data with useful energy as the independent variable, all the neutron data appear consistent with the anticipated $\langle \cos \theta \rangle$ dependence of the exploding pusher's yield. The implied reduced ion temperatures associated with these

degraded yields were also measured to be consistent as seen in Figures 1 and 5. The significantly reduced thermonuclear gains correspond to the non-optimum matching between the incident pulse and the target geometry parameters as anticipated.

Finally interesting results were obtained concerning the net energy change experienced by the 3.52 MeV alpha particles born within the core of the compressed target as a results of the thermonuclear event. The energy spectra of the alpha particles were determined by time-of-flight techniques using magnetic spectrometers for both the short and long pulse experiments. As indicated in Figure 1 and summarized in Figure 6, the net change in the alpha's energy is seen to be a function of pulse width. In short pulse experiments, the peak of the alpha particle distribution suffers approximately a 250 keV energy loss in traversing the ρr of the fuel and the pusher. On the other hand, net energy gains are observed on several long pulse experiments. Estimating the thermonuclear burn time using the simple exploding pusher scaling model outlined in Figure 5, and estimating the alpha transit time from the core to the outer absorbing coronal region assumed to be at the initial radius of the microsphere, results in Figure 6 depicting the observed shift in alpha particle energy as function of when in time it passes through the targets' corona with respect to the incident Gaussian laser pulse. One observes that only for those cases wherein the alphas exit at a time substantially near the peak of the incident pulse, does one record an upshifted alpha distribution peak. It is postulated that those upshifts are due to an electrostatic acceleration, of sorts, as the alpha particles traverse the regions near critical wherein the on going absorption processes have generated intensity dependent electric fields.

An initial attempt to estimate this postulated intensity dependence is illustrated in Figure 7. The net alpha acceleration, assuming constant ρr losses

for all the data, is plotted against an "effective" laser intensity at the alpha particle coronal transit time. (ΔE_α) P_r equal to -240 keV represents the main energy loss for the short pulse experiments with -400 keV equal to the maximum loss observed in the data set. The "effective" laser intensity equals the peak Gaussian laser intensity reduced by the fraction indicated by the relative timing between the alpha transit and peak laser power times. Energy gains scaling with the .5 to 1.0 power of the effective laser intensity are implied. Implications of these results with respect to suggested laser-plasma absorption mechanisms are presently being examined.

Reference to a company or product names does not imply approval or recommendation of the product by the University of California or the U.S. Department of Energy to the exclusion of others that may be suitable.

NOTICE

"This report was prepared as an account of work sponsored by the United States Government. Neither the United States nor the United States Department of Energy, nor any of their employees, nor any of their contractors, subcontractors, or their employees, makes any warranty, express or implied, or assumes any legal liability or responsibility for the accuracy, completeness or usefulness of any information, apparatus, product or process disclosed, or represents that its use would not infringe privately-owned rights."

LARGE DIAMETER, LONG PULSE MICROSPHERE IMPLOSION EXPERIMENTS



	Short Pulse, Small Diameter	Long Pulse, Large Diameter
Target and laser parameters	85 μm^D , 0.8 μm wall, 2 mg/cc 120 J, 40 ps, 3 TW	150 μm^D , 1.0 μm wall, 2 mg/cc 550 J, 150 ps, 3.8 TW
Absorption fraction	22%	10%
Yield ratio	2×10^{-6}	6×10^{-8}
Alpha and proton energy shifts	-250 keV (He^4) -100 keV (D-D)	+300 keV (He^4) +200 keV (D-D)
Backscattered spectrum	—	~80% red shifted
Ion temp.	5-6 keV	3-3.5 keV

Figure 1

MICROSPHERE TARGETS ABSORB LESS AT LONGER PULSES

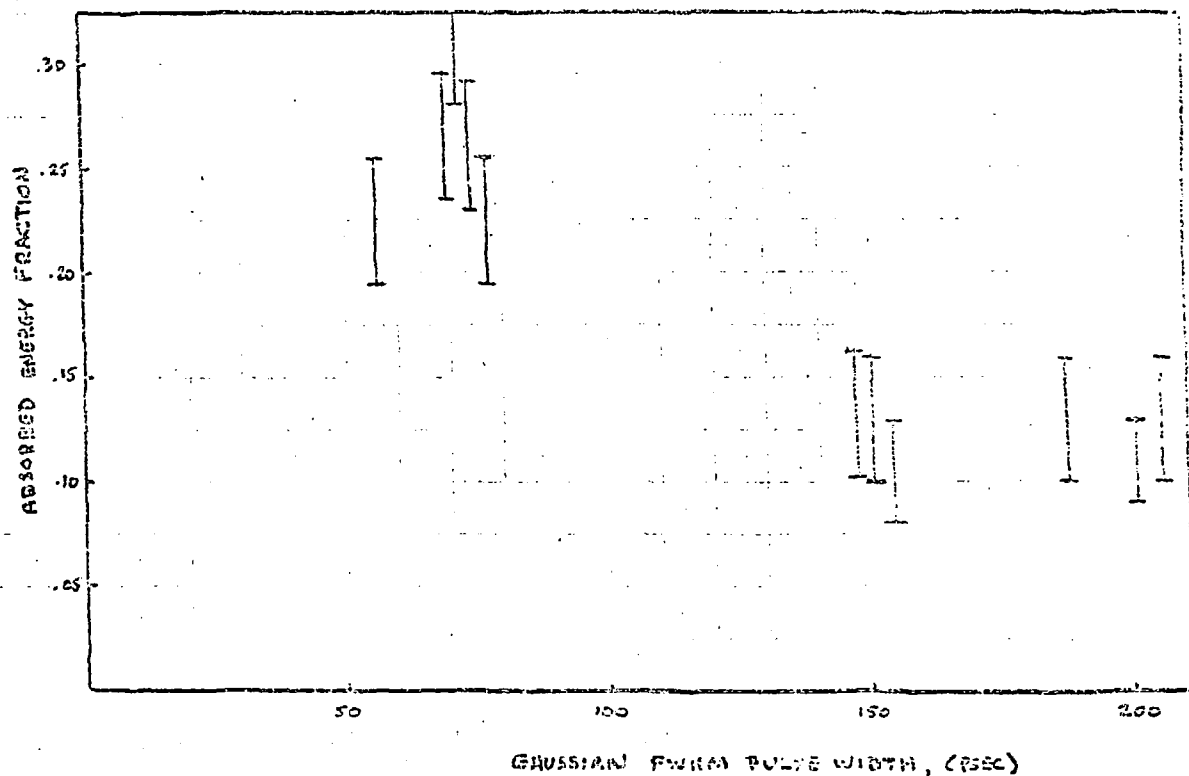
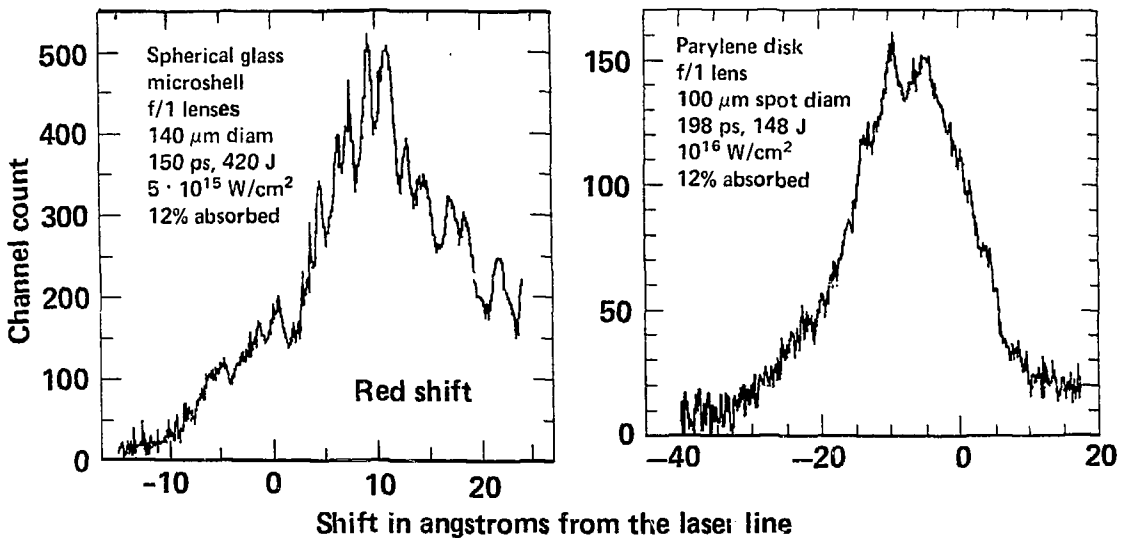
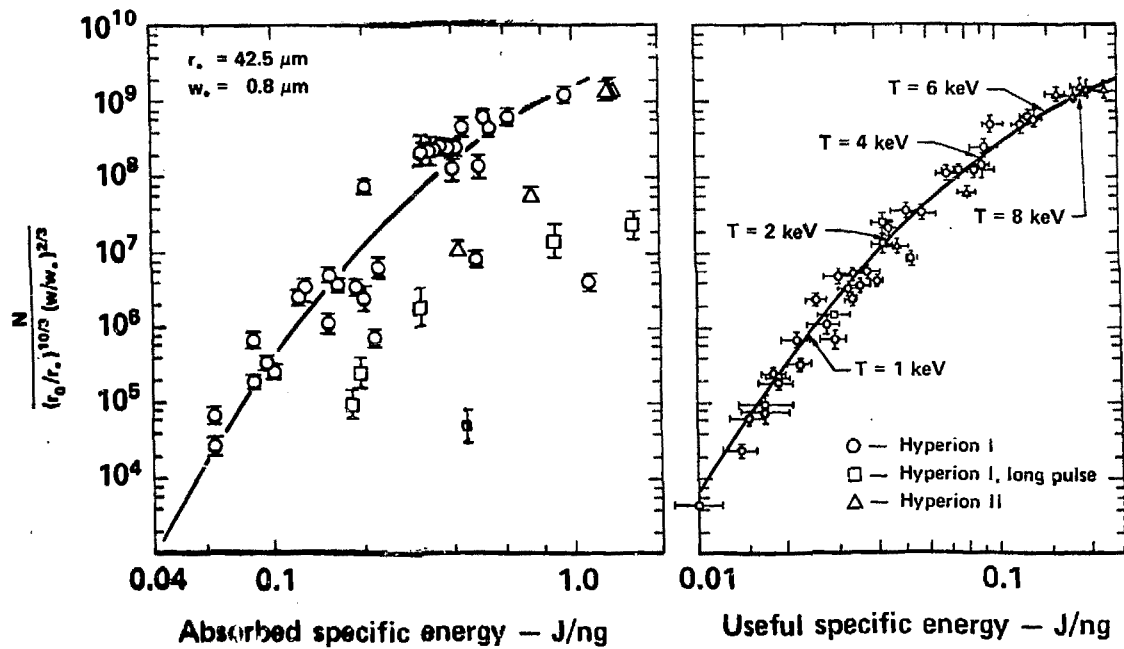


Figure 2

THE SPECTRUM OF THE BACK-REFLECTED LIGHT BROADENS AND SHIFTS TO THE RED IN LARGE SPOT, LONG PULSE, HIGH INTENSITY EXPERIMENTS



NEUTRON YIELDS SCALE WITH "USEFUL" RATHER THAN
ABSORBED SPECIFIC ENERGY



SIMPLE SCALING MODEL



$$N \cong n_D n_T \langle \sigma v \rangle V t \sim n_0^2 R_0^4 C^{2/3} \langle \sigma v \rangle T_{ion}^{-1/2}$$

Assuming $C \sim \frac{w}{R_0 n_0}$

Then for fixed DT fill

$$N = 8.6 \times 10^6 R_0^{10/3} w^{2/3} \epsilon_c^{-7/6} \exp(-5.45 \epsilon_c^{-1/3})$$

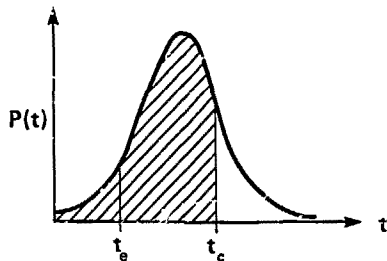
$$T_{ion} \sim E_c / M_p = \epsilon_c$$

Here

R_0 = Initial microshell radius in μm
 w = Initial microshell wall thickness in μm
 M_p = 1/2 the initial shell mass in ng
 E_c = The useful fraction of the absorbed energy in J

$$E_c = \frac{1}{8} \int_{-t_e}^{t_e} \eta P(t) dt + \frac{1}{8} \int_{t_e}^{t_c} \eta P(t) dt$$

explosion phase acceleration phase



η = fractional absorption
 t_e = time required for shockwave to penetrate shell
 $t_c - t_e$ = time required for pusher to traverse $\sim 25\%$ of R_0

ALPHA PARTICLE ENERGIES AS A FUNCTION OF PULSE DURATION

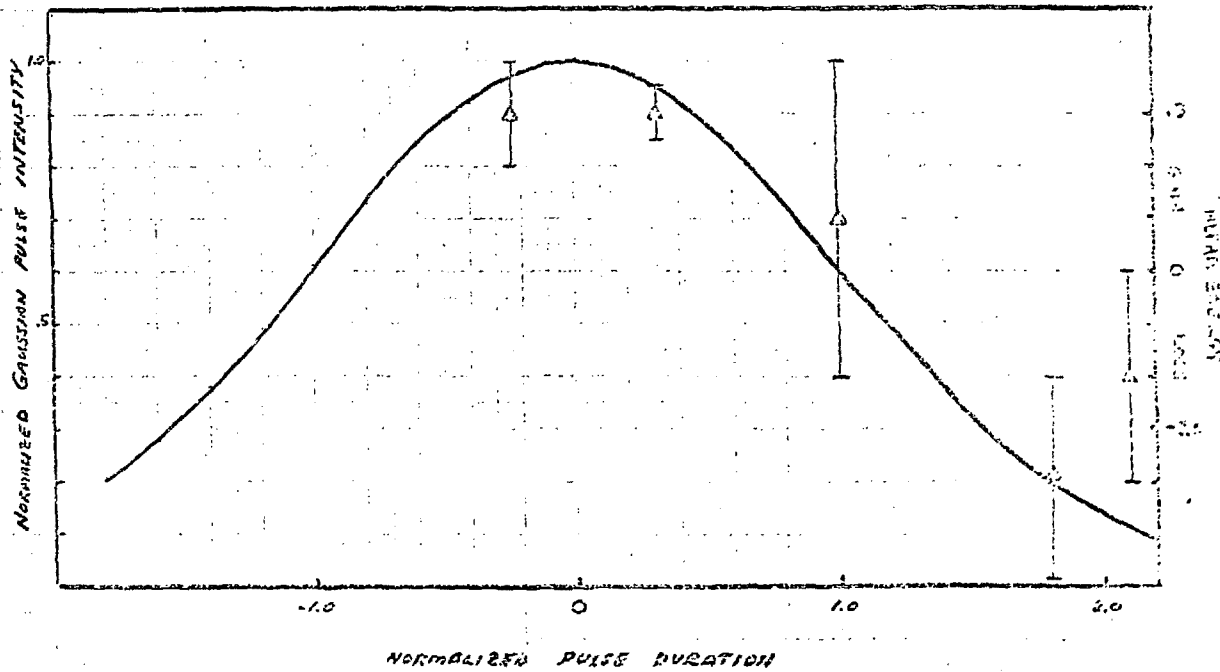


Figure 6

Thermonuclear Alpha Particles are Upshifted in Energy
with Increasing Effective Laser Intensity

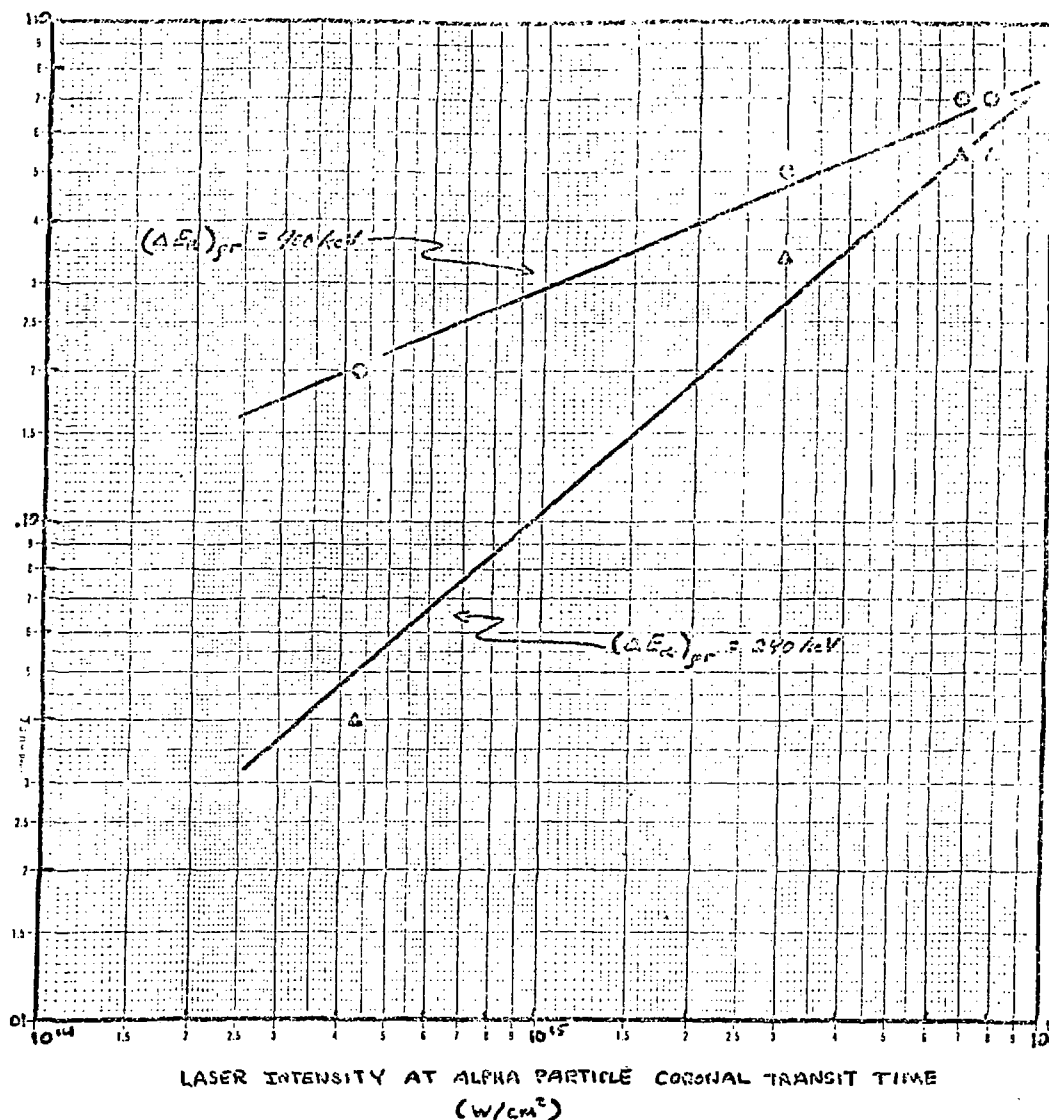


Figure 7